Linear and nonlinear waves in surface and wedge index potentials

Nikolaos K. Efremidis,[1,*] Dimitrios G. Papazoglou,[2,3] and Stelios Tzortzakis[2,3]

[1]*Department of Applied Mathematics, University of Crete, 71409, Heraklion, Crete, Greece*

[2]*Institute of Electronic Structure and Laser, Foundation for Research and Technology-Hellas, 71110, Heraklion, Greece*

[3]*Materials Science and Technology Department, University of Crete, P.O. Box 2208, 71003, Heraklion, Greece*

**Corresponding author: nefrem@tem.uoc.gr*

Received December 16, 2011; revised March 9, 2012; accepted March 12, 2012;
posted March 14, 2012 (Doc. ID 160167); published May 21, 2012

We study optical beams that are supported at the surface of a medium with a linear index potential and by a piecewise linear wedge-type potential. In the linear limit the modes are described by Airy functions. In the nonlinear regime we find families of solutions that bifurcate from the linear modes and study their stability for both self-focusing and self-defocusing Kerr nonlinearity. The total power of such nonlinear waves is finite without the need for apodization.

OCIS codes: 190.4350, 190.3270, 050.1940, 350.5500.

Over the past years there is a significant amount of activity in studying Airy beams in optics [1,2]. Waves of the Airy type are the only nondiffracting solutions of the paraxial equation in one dimension that ideally carry infinite power and propagate along parabolic trajectories. Note that, in two dimensions, families of parabolic waves also exhibit similar properties [3]. In optics, Airy waves are associated with applications such as particle manipulation [4], filament generation [5], optical bullet formation [6,7], and abrupt autofocusing [8–11]. Nonlinear properties of Airy waves have also been studied theoretically and experimentally [12–16].

In the presence of a linear refractive index potential, the transverse velocity of the Airy wave can become zero [17–19]. If, in addition, a Dirichlet (zero) boundary condition is imposed, then finite power stationary Airy wave solutions exist that are truncated at the zeros of the Airy function [20]. In quantum mechanics, such solutions are interpreted as the eigenfunctions of a particle that is bouncing under the action of a constant gravitational force [21]. The optical analogue of such a phenomenon is described by an optical wave propagating at the surface of a medium with an additional linear index potential.

In this work we study such optical waves propagating in linear index potentials at the surface of a medium as well as in piecewise linear wedge-type potentials. We consider the case of a nonlinear medium with either self-focusing (SF) or self-defocusing (SDF) nonlinearity. We find that the families of the supported SF waves exhibit stable dynamics. In addition, we observe the transition from Airy waves in the linear limit, to π-out-of-phase soliton bound states in the strongly nonlinear case. For SDF nonlinearity, the first family of solutions is stable, while higher-order families have a complicated stability structure with alternating regions of stability and instability as a function of the propagation constant.

In the paraxial limit, the evolution of the optical field is described by the following nonlinear Schrödinger (NLS)-type equation:

$$i\psi_z + (1/2)\psi_{xx} - V(x)u + \gamma|\psi|^2\psi = 0. \tag{1}$$

Equation (1) is normalized, ψ is the field amplitude, x is the transverse and z is the propagation coordinate, $V(x)$ is the potential [$-V(x)$ describes the index contrast], and $\gamma = \pm 1$. In Eq. (1), x, z_0, $V(x)$, and $|\psi|^2$ scale as x_0, z_0, $1/(k_0^2 x_0^2 n_0)$, and $1/(k_0^2 x_0^2 n_0 n_2)$, respectively, where $k_0 = 2\pi/\lambda$, λ is the wavelength, n_0 is the refractive index, and n_2 is the Kerr coefficient.

In the linear limit ($\gamma \to 0$) and in the presence of a continuous piecewise linear wedge potential of the form

$$V(x) = \begin{cases} \frac{d_1 x}{2} & x < 0 \\ \frac{d_2 x}{2} & x > 0 \end{cases}, \tag{2}$$

where d_1, d_2 are real numbers, Eq. (1) supports stationary solutions. In general, these solutions are expressed in terms of Airy functions (Ai and Bi). However, limiting ourselves to trapping potentials [such that $V(x)$ goes to infinity as $x \to \pm\infty$], the solutions take the form of Airy Ai functions, i.e.,

$$\psi_j(x,z) = A_j \mathrm{Ai}[\sigma_j |d_j|^{1/3}(x - c_j)] e^{-i(d_j c_j/2)z}, \tag{3}$$

where $j = 1$ ($j = 2$) for $x < 0$ ($x > 0$), respectively, and $\sigma_j = \mathrm{sgn}(d_j)$. The parameters of Eq. (3) are determined from the continuity of ψ and ψ_x at $x = 0$:

$$c_1 d_1 = c_2 d_2, \tag{4}$$

$$A_1 \mathrm{Ai}(\xi_1) = A_2 \mathrm{Ai}(\xi_2), \tag{5}$$

$$\sigma_1 |d_1|^{1/3} A_1 \mathrm{Ai}'(\xi_1) = \sigma_2 |d_2|^{1/3} A_2 \mathrm{Ai}'(\xi_2), \tag{6}$$

where $\xi_j = -\sigma_j |d_j|^{1/3} c_j$. Combining Eqs. (4)–(6), we find $\sigma_1 |d_1|^{1/3} \mathrm{Ai}(\xi_2)\mathrm{Ai}'(\xi_1) = \sigma_2 |d_2|^{1/3} \mathrm{Ai}(\xi_1)\mathrm{Ai}'(\xi_2)$, which, upon substitution of Eq. (4), can be solved for the discrete set of values of c_1. Subsequently, c_2 and A_2 are determined as a function of c_1 and A_1 (which is chosen arbitrarily) from either Eqs. (4) and (5) [if $\mathrm{Ai}(\xi_j) \neq 0$] or from Eqs. (4) and (6) [if $\mathrm{Ai}(\xi_j) = 0$]. Two different classes of trapping potentials are depicted in Fig. 1. If $d_1 < 0$ and $d_2 > 0$, the resulting wedge-type potential supports an infinite discrete set of modes with finite power

0146-9592/12/111874-03$15.00/0

[Fig. 1(a)]. The two Airy functions composing the wave have opposite directions with their oscillating parts facing inward. A particularly interesting class of solutions are surface waves at the interface of a high-index medium ($x > 0$) with an index gradient d_2 and a low-index medium ($x < 0$) and no index gradient. We can describe this system in the semi-infinite line $x > 0$ with Dirichlet boundaries $\mathrm{Ai}(\xi_2) = 0$. When $d_2 > 0$, the potential is trapping, the oscillating part of the Airy wave is facing toward the interface, and, thus, the power of the wave is finite. Surface modes are also supported if $d_2 < 0$, however, such waves carry infinite power.

By increasing the intensity of the optical beam, nonlinear effects become important. We are going to study the bifurcations and the stability of families of nonlinear waves that are supported by Kerr SF ($\gamma = 1$) and SDF ($\gamma = -1$) nonlinearity. We assume that Eq. (1) supports stationary solutions of the form $\psi(x, z) = u(x)e^{ikz}$; thus

$$-ku + (1/2)u'' + V(x)u + \gamma u^3 = 0. \tag{7}$$

Equation (7) has the form of a second Painlevè transcendent in the regions $x > 0$ and $x < 0$. Using a Newton iteration scheme, we numerically solved Eq. (7) and found families of stationary solutions. In particular, from each linear Airy-type mode, a family of solutions bifurcates, i.e., the nth family of solutions bifurcates from the nth Airy mode. We focus our attention on the two types of potentials depicted in Fig. 1, where, for simplicity, $d_2 = -d_1 = 1$. We find families of nonlinear localized solutions and study their stability independently using two different approaches: Direct numerical simulations using a split-step Fourier method and linear stability analysis. According to this latter approach,

$$\psi(x, z) = [u(x) + A(x, z) + iB(x, z)]e^{ikz}, \tag{8}$$

where the perturbations A and B are real functions. The resulting linearized system reads $A_z = L_0 B$, $B_z = -L_1 A$, where $L_0 = k - (1/2)\partial_{xx} - u^2$ and $L_1 = k - (1/2)\partial_{xx} - 3u^2$. Assuming that $(A, B) = e^{i\lambda z}(A_0(x), B_0(x))$ and numerically solving, using finite differences, the eigenvalue problem, we can determine the linear stability of the stationary solutions.

Typical amplitude profiles belonging to the families 1, 4, and 8 in the presence of SF nonlinearity are depicted in Figs. 2(a)–2(c). By increasing the value of the propagation constant k, the maximum intensity of the beam increases and its width decreases. Eventually, for very high intensities, the last (nonlinear) term in Eq. (7) dominates over the linear potential term, and the solution asymptotically takes the form of an NLS soliton (the first family of solutions) or a sequence of π-out-of-phase solitons (the higher-order families of solutions). Considering the stability of such SF surface waves, our numerical simulations show that they are stable independently of the mode number and k. However, some moderate instabilities are observed in the case of high-order families and for particular ranges of values of the propagation constant k. In particular, we observe that the straight trajectory of the wave is slightly perturbed as it propagates. Such oscillations are persistent along z, but do not grow or destabilize the wave itself. Furthermore, the amplitudes of these oscillations are small and, thus, they are hardly noticeable in the beam dynamics.

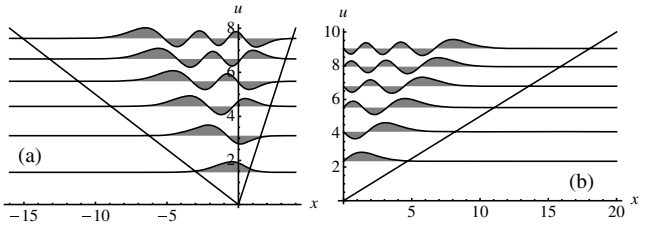

Fig. 1. Linear mode profiles for (a) a wedge potential with $d_1 = -1$, $d_2 = 4$, (b) linear potential at the surface of a semi-infinite medium with $d_2 = 1$. In both cases, the first six modes are depicted.

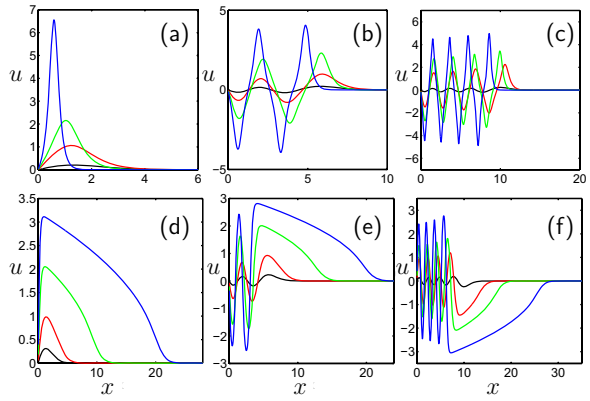

Fig. 2. (Color online) Typical amplitude profiles of nonlinear waves supported at the surface of a Kerr nonlinear medium. In (a), (b), and (c) SF; and in (d), (e), and (f) SDF amplitude profiles belonging to the families 1, 4, and 8 are shown, respectively.

Typical amplitude profiles in the case of SDF nonlinearity are shown in Fig. 2(d)–2(f). As the propagation constant k decreases, the maximum intensity and total power of the surface mode increases [Fig. 3(a)]. In addition, the width of the first lobe expands significantly as k decreases with an amplitude that gradually goes to zero with x. On the other hand, as k decreases, the width of the subsequent oscillations remain almost constant with a slight tendency to decrease.

In the case of SDF nonlinearity, the first family of solutions is always stable. However, by applying a linear stability analysis, we found that higher-order modes have both regions of stability and instability, depending on the value of k. For example, in the case of the fourth family of solutions, in Fig. 3(a), we see such a complicated stability structure with alternating regions of stability and instability [$G = \max(\mathrm{Im}(\lambda_j))$ is the growth rate]. These results are in agreement with those of direct numerical simulations. In particular, in Figs. 3(b) and 3(f), we see examples of stable surface modes. In Fig. 3(c), an unstable wave is depicted [a more detailed plot of the same simulation is shown in Fig. 3(d)]. We notice that, originally, the beam propagates in an almost stable fashion. However, it gradually starts "breathing," and these oscillations become larger with z. However, after some point, the breathing, instead of completely disintegrating the beam, starts to decrease, leading to the revival of the initial

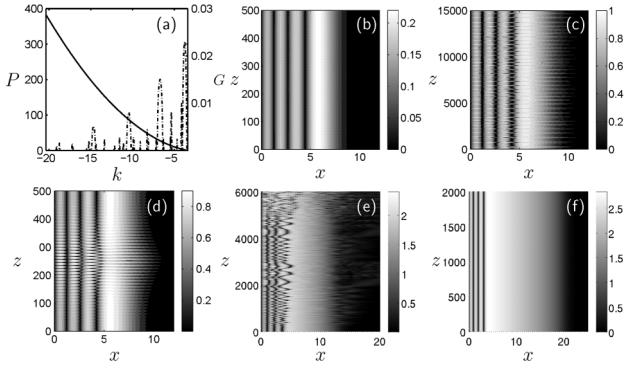

Fig. 3. (a) Power P (solid curve) and growth rate G (dashed–dotted curve) as a function of the propagation constant k of the fourth family of surface waves in the presence of SDF nonlinearity. Corresponding dynamics for (b) $k \approx -3.42$, (c) $k \approx -3.94$ [(d) shows details of the same simulation], (e) $k \approx -6.54$, and (f) $k \approx -10.1$.

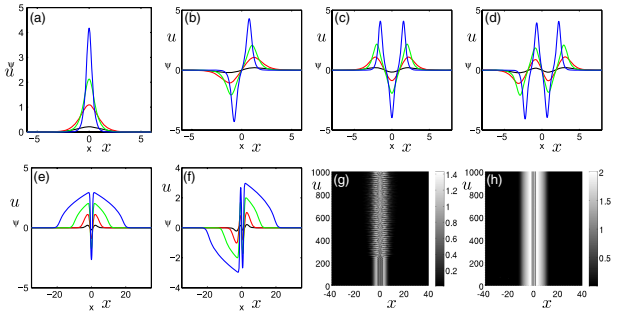

Fig. 4. (Color online) Typical amplitude profiles supported by a wedge index potential in the case of (a)–(d) families 1–4 in a SF medium, and (e)–(f) families 3 and 4 in a SDF medium. (g) Unstable and (h) stable dynamics of beams belonging to the fourth SDF family.

beam profile. Such oscillations happen quasi-periodically along z. Our numerical simulations show that, in most of the cases, such instabilities do not disintegrate the surface wave but lead to dynamics similar to what we just described. However, in a few cases, such as the one shown in Fig. 3(e), the growth rate is large enough and the wave eventually disintegrates.

In the case of symmetric wedge potentials $d_2 = -d_1 = 1$, $u(x)$ is either even $u(-x) = u(x)$ or odd $u(-x) = -u(x)$. Typical amplitude profiles of nonlinear wedge profiles are shown in Figs. 4(a)–4(f). Our simulations show that, independent of the mode number and k, such families of solutions are stable if the nonlinearity is SF. The stability of SDF wedge families is more complicated. As in the case of surface beams, the first family is always stable, while higher-order families are characterized by alternating regions of stability and instability in the $G - k$ diagrams. For example, in Fig. 4, we see typical propagation dynamics of an unstable [Fig. 4(g)] and a stable [Fig. 4(h)] SDF wave belonging to the fourth family of solutions.

In conclusion, we have studied linear and nonlinear waves supported by linear surface and wedge-type index potentials and have analyzed their stability. More importantly, independent of the type of the nonlinearity and the potential, such families of solutions can be stable and thus experimentally observable using, for example, intense femtosecond lasers (see, e.g., [7]). Assuming typical values for an AlGaAs medium, $\lambda_0 = 1\ \mu$m, $x_0 = 15\ \mu$m, and $n_0 = 3.5$, nonlinear effects can become appreciable for a peak intensity of the order of 10 MW/cm^2 and total power of the order of 10 kW.

N. K. Efremidis is partially supported by the European Union's Seventh Framework Programme (FP7-REGPOT-2009-1) project "Archimedes Center for Modeling, Analysis and Computation" under grant agreement no. 245749.

References

1. G. A. Siviloglou and D. N. Christodoulides, Opt. Lett. **32**, 979 (2007).
2. G. A. Siviloglou, J. Broky, A. Dogariu, and D. N. Christodoulides, Phys. Rev. Lett. **99**, 213901 (2007).
3. M. A. Bandres, Opt. Lett. **33**, 1678 (2008).
4. J. Baumgartl, M. Mazilu, and K. Dholakia, Nat. Photon. **2**, 675 (2008).
5. P. Polynkin, M. Kolesik, J. V. Moloney, G. A. Siviloglou, and D. N. Christodoulides, Science **324**, 229 (2009).
6. A. Chong, W. H. Renninger, D. N. Christodoulides, and F. W. Wise, Nat. Photon. **4**, 103 (2010).
7. D. Abdollahpour, S. Suntsov, D. G. Papazoglou, and S. Tzortzakis, Phys. Rev. Lett. **105**, 253901 (2010).
8. N. K. Efremidis and D. N. Christodoulides, Opt. Lett. **35**, 4045 (2010).
9. D. G. Papazoglou, N. K. Efremidis, D. N. Christodoulides, and S. Tzortzakis, Opt. Lett. **36**, 1842 (2011).
10. P. Zhang, J. Prakash, Z. Zhang, M. S. Mills, N. K. Efremidis, D. N. Christodoulides, and Z. Chen, Opt. Lett. **36**, 2883 (2011).
11. I. Chremmos, N. K. Efremidis, and D. N. Christodoulides, Opt. Lett. **36**, 1890 (2011).
12. J. Giannini and R. Joseph, Phys. Lett. A **141**, 417 (1989).
13. T. Ellenbogen, N. Voloch-Bloch, G.-P. Ayelet, and A. Arie, Nat. Photon. **3**, 395 (2009).
14. R.-P. Chen, C.-F. Yin, X.-X. Chu, and H. Wang, Phys. Rev. A **82**, 043832 (2010).
15. I. Kaminer, M. Segev, and D. N. Christodoulides, Phys. Rev. Lett. **106**, 213903 (2011).
16. Y. Fattal, A. Rudnick, and D. M. Marom, Opt. Express **19**, 17298 (2011).
17. W. Liu, D. N. Neshev, I. V. Shadrivov, A. E. Miroshnichenko, and Y. S. Kivshar, Opt. Lett. **36**, 1164 (2011).
18. N. K. Efremidis, Opt. Lett. **36**, 3006 (2011).
19. Z. Ye, S. Liu, C. Lou, P. Zhang, Y. Hu, D. Song, J. Zhao, and Z. Chen, Opt. Lett. **36**, 3230 (2011).
20. O. Valleé and M. Soares, *Airy Functions and Applications to Physics* (World Scientific, 2004).
21. D. M. Greenberger, Am. J. Phys. **48**, 256 (1980).